Journal of Science and Technology in Civil Engineering, HUCE (NUCE), 2021, 15 (4): 136–147

INVESTIGATION OF THE EFFECTS OF OPENING SIZE AND LOCATION ON PUNCHING SHEAR RESISTANCE OF FLAT SLABS USING ABAQUS

Nguyen Tuan Trung[a,*], Pham Thanh Tung[a]

[a] *Faculty of Building and Industrial Construction, Hanoi University of Civil Engineering, 55 Giai Phong road, Hai Ba Trung district, Hanoi, Vietnam*

Article history:
Received 12/8/2021, Revised 20/9/2021, Accepted 01/10/2021

Abstract

The paper presents a numerical study on the effects of opening size and location on punching shear resistance of flat slabs without drop panels and shear reinforcement using ABAQUS. The study proposes an ABAQUS model that is enable to predict the punching shear resistance of flat slabs with openings. The model is validated well with the experimental data in literature. Using the validated numerical model, the effects of opening size and location on the punching shear resistance of flat slabs are then investigated, and the numerical results are compared with those predicted by ACI 318-19 and TCVN 5574:2018. The comparison between experimental and numerical results shows that the ABAQUS model is reliable. The punching shear resistances calculated by ACI 318-19 and TCVN 5574:2018 with different opening sizes and locations are agreed well to each other, since the design principles between two codes now are similar.

Keywords: flat slabs; punching shear; slab opening; shear resistance; ABAQUS.

https://doi.org/10.31814/stce.huce(nuce)2021-15(4)-12

1. Introduction

Flat slab systems are widely used worldwide and in Vietnam since they have numerous advantages. In the flat slab systems, the governing failure mode is punching shear failure caused by high shear stresses in the slab-column connection area. This type of shear failure mode is characterized by the formation of a cone-shaped element, and it is a brittle failure. Punching shear behaviour of flat slabs has been examined by numerous researchers through experimental and analytical studies [1–3]. A brief review of punching shear in slabs without shear reinforcement is summarised by Elstner and Hognestad [4] and Moe [5]. Their experimental work is the basis for the ACI design approach [6]. The existing punching shear testing database, even though it is large [1–6], cannot address all aspects of punching shear stress transfer mechanisms. Recently, with the development of finite element method, in modern research in structural engineering, the finite element analyses (FEA) are essential for supplementing experimental research. This method can provide insights into structural behavior, and, in the case herein, on punching shear transfer mechanisms.

On the other hand, openings are usually arranged next to the columns to provide adequate space for mechanical and electrical purposes. In reinforced concrete (RC) flat slabs, if the openings are

[*]Corresponding author. *E-mail address:* trungnt2@nuce.edu.vn (Trung, N. T.)

positioned closed to the column, the punching shear stresses are increased and thus the punching shear capacity will drastically reduce. Therefore, it is vital to study this issue to understand the behaviour and to accurately calculate the punching shear stresses of flat slabs with various sizes and locations of the opening. Genikomsou and Polak [7, 8] conducted the experimental and numerical studies on the effect of opening on RC flat slabs. Mostofinejad et al. [9] also studied the effect of opening on the punching shear behaviour by the numerical analyses using ANSYS.

Many researches are also conducted in Vietnam to study the punching shear behaviour of flat slabs. Hieu [10] conducted an experimental study on punching shear resistance of ultra high performance concrete flat slabs. Vuong [11] studied the behaviour of flat slabs and their punching shear resistance with different boundary conditions using ANSYS. Tam [12] studied the punching shear behaviour of prestressed RC flat slabs. The author conducted an extensive experimental study, numerical analyses using ANSYS, and proposed an analytical model to predict the punching shear resistance of prestressed flat slabs. Vinh [13] compares the punching shear resistance of two-way RC slabs without transverse reinforcement with different building codes. Few researches used ABAQUS to study the behaviour of composite columns [14, 15]. However, no study has been conducted yet in Vietnam to investigate the effect of opening dimension and location on the punching shear resistance of flat slabs; although the current RC design code TCVN 5574:2018 [16] has implemented new regulations to take account of this problem in design. Therefore, a study on this issue is urgently needed.

This paper aims to propose an Abaqus numerical model to study the effect of opening dimension and location on the punching shear resistance of flat slabs without drop panels and shear reinforcement. Firstly, the design equations recommended by ACI 318-19 [6] and TCVN 5574:2018 are described. Secondly, the methodology and the material models used in the analyses are presented. Thirdly, the FE model is calibrated and validated with an available experimental study in literature. Using the validated model, a parametric study is conducted to investigate the effect of opening with different dimension and location on the punching shear resistance of flat slabs, while comparing to those values obtained by ACI 318-19 and TCVN 5574:2018.

2. Design provisions of punching shear resistance according to TCVN 5574:2018 and ACI 318-19

2.1. *TCVN 5574:2018*

TCVN 5574:2018 stipulates that the slabs without shear reinforcement subjected to a uniformly distributed load over an area need to be checked with punching shear by Eq. (1).

$$F \leq F_{b,u} = R_{bt} u h_0 \tag{1}$$

where: F is the concentrated force caused by external loads; $F_{b,u}$ is the punching shear resistance of concrete; u is the perimeter of the critical section; h_0 is the effective depth.

When determining u, it is needed to consider the critical section at a distance of $0.5h_0$ from the column edges (Fig. 1), where there is shear stress caused by shear force Q and connection moment M.

If shear reinforcement is provided within the punching shear cone, the shear resistance is checked using Eq. (2).

$$\begin{aligned} F &\leq F_{b,u} + F_{sw,u} \\ F_{sw,u} &= 0.8 \frac{R_{sw} A_{sw}}{s_w} u \end{aligned} \tag{2}$$

but not greater than $2F_{b,u}$; A_{sw} is area of shear reinforcement; s_w is spacing of shear reinforcement.

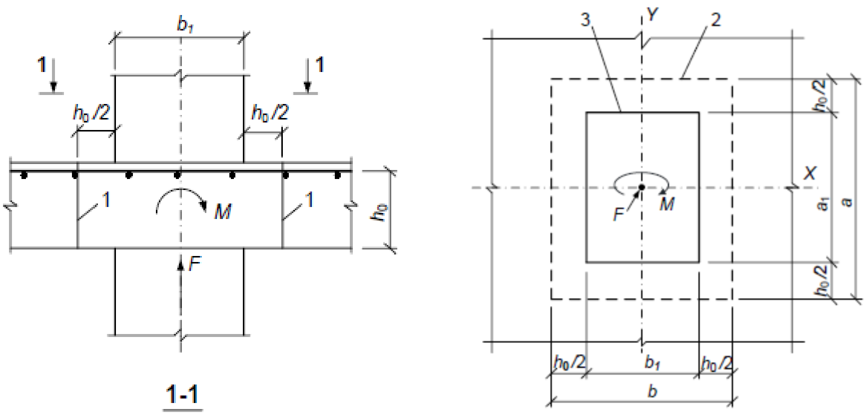

1- Calculated cross section; 2- Perimeter of the calculated cross section; 3- Perimeter of the load-transferred area

Figure 1. Calculation diagrame of punching shear resistance without shear reinforcement

The punching shear resistance of concrete $F_{b,u}$ is taken as in Eq. (1), and $F_{sw,u}$ is total shear resistance due to shear reinforcement around the critical perimeter. The value of R_{sw} can only be taken up to 300 MPa as maximum. Shear reinforcement is taken into account when $F_{sw,u}$ is not smaller than $0.25F_{b,u}$.

A novelty of TCVN 5574:2018 compared to TCVN 5574:2012 [17] is that TCVN 5574:2018 proposes the stipulations to check of punching shear resistance with combined shear force and bending moment at connections and with openings existed in flat slabs near the concentrated force. This is considered as a significant improvement of TCVN 5574:2018.

Under the combined effect of shear force F and bending moment M, TCVN 5574:2018 requires that sum of the ratios $F/F_{b,u}$ and $M/M_{b,u}$ shall be smaller than 1.0, where $M_{b,u}$ is the moment resistance of the critical section.

If there is an opening at a distance from edge of the opening to edge of the loaded area not greater than $6h_0$, the effective control perimeter shall be reduced by an ineffective perimeter which lies in between two tangents drawn to the outline of the opening from the center of the loaded area (Fig. 2).

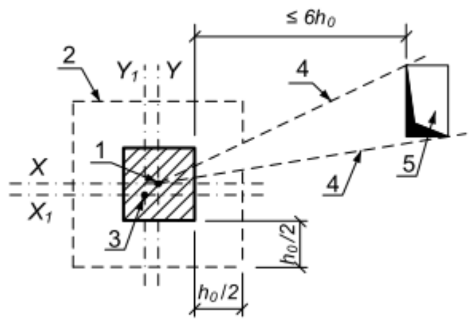

1- centroid of load transferred area; 2- unclosed effective control perimeter; 3- centroid of effective control perimeter; 4- two tangents drawn to the outline of the opening from the center of the loaded area (top surface of column); 5- opening

Figure 2. Critical perimeter near opening according to TCVN 5574:2018

2.2. ACI 318-19

According to ACI 318-19, the basic equation for shear design states that:

$$V_u \leq \phi V_n \tag{3}$$

where V_u is the factored shear force due to the loads; ϕ is the strength reduction factor, taken as 0.75 (Table 21.2.1 ACI 318-19).

V_n is the nominal shear resistance of the slab, determined by Eq. (4).

$$V_n = V_c + V_s \tag{4}$$

where V_c and V_s are the shear resistances attributed to the concrete and the shear reinforcement, respectively.

ACI 318-19 adopts the critical shear perimeter at a distance $d/2$ from the loaded area (column) as shown in Fig. 3, where d is the effective depth of the slab.

For two-way shear, V_c is taken as the smallest of (5), (6) and (7)

$$V_c = 0.33\lambda_s\lambda\sqrt{f'_c}b_0 d \tag{5}$$

where λ_s is size effect modification factor: $\lambda_s = \sqrt{2/(1+0.004d)} \leq 1; b_0$ is perimeter of critical section; λ is modification factor depending on normal or lightweight concrete, taken as 1.0 for normal concrete.

$$V_c = \left(0.17 + \frac{0.33}{\beta}\right)\lambda_s\lambda\sqrt{f'_c}b_0 d \tag{6}$$

where β is the ratio of long side to short side of column (or loaded area).

$$V_c = \left(0.17 + \frac{0.083\alpha_s d}{b_0}\right)\lambda_s\lambda\sqrt{f'_c}b_0 d \tag{7}$$

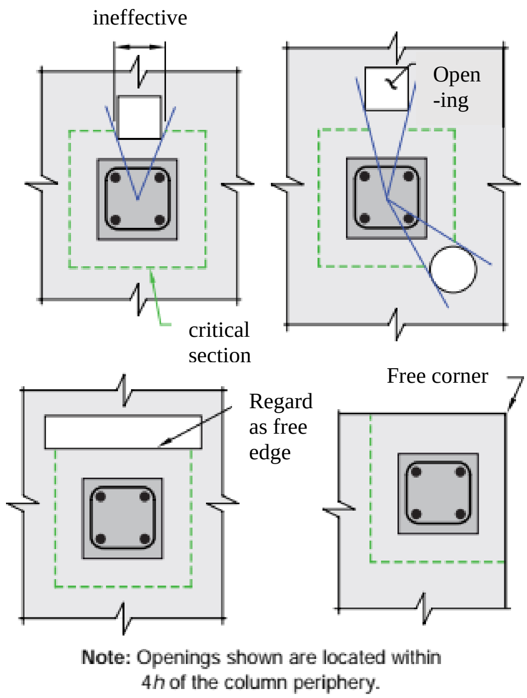

Figure 3. Critical perimeter near opening according to ACI 318-19

where α_s is 40 for interior columns, 30 for edge columns, and 20 for corner columns.

When the factored shear stress v_u is greater than shear resistance ϕv_c, shear reinforcement requires. ACI 318-19 specifies that it provides shear reinforcement in the slab if its effective depth $d \geq 150$ mm, but not smaller than 16 times of diameter of shear reinforcement. If using stirrups, V_n shall not be greater than $0.5\sqrt{f'_c}b_0 d$ and V_c shall not be greater than $0.17\lambda_s\lambda\sqrt{f'_c}b_0 d$. Therefore, V_s is not greater than $0.33\lambda_s\lambda\sqrt{f'_c}b_0 d$. If shear reinforcement is arranged perpendicular to the member axis, V_s is calculated by Eq. (8).

$$V_s = \frac{A_v f_y d}{s} \tag{8}$$

where s is stirrup spacing; A_v is total shear reinforcement area; f_y is yield stress of reinforcing steel.

When there is opening near the loaded area (column), the critical perimeter is reduced depending on the size and the location of the opening. The ineffective perimeter is a part of the critical perimeter contained between two tangents drawn to the outline of the opening from the center of the loaded area (top surface of column). ACI 318-19 considers the reduction in the critical perimeter if the shortest distance between the perimeter of the loaded area (column) and the edge of the opening is smaller or equal to $4h$, where h is the slab thickness (Fig. 3).

3. Finite element simulation

Simulation of the proposed numerical model is presented in this section in terms of the methodology and the material models of concrete and reinforcement. The test data from the literature is used for validation. The numerical results are compared to the test results regarding of deflections, strength and crack patterns.

3.1. Previous test data used for model validation

This research uses the experimental data studied on punching shear resistance of flat slabs with openings conducted by Genikomsou và Polak [7]. They conducted a series of test specimens with slab openings and no shear reinforcement. The specimens were isolated slab-column connections, loaded through the column. They were simply supported along the edges, represented the lines of contra flexure in the parent slab-column system. To do so, thick neoprene pads were provided on top and bottom of the slab to allow rotations. The neoprene pads were about 25 mm thick and 50 mm wide installed along the supporting lines. All specimens had the same dimensions (1800×1800×120 mm) as shown in Fig. 4.

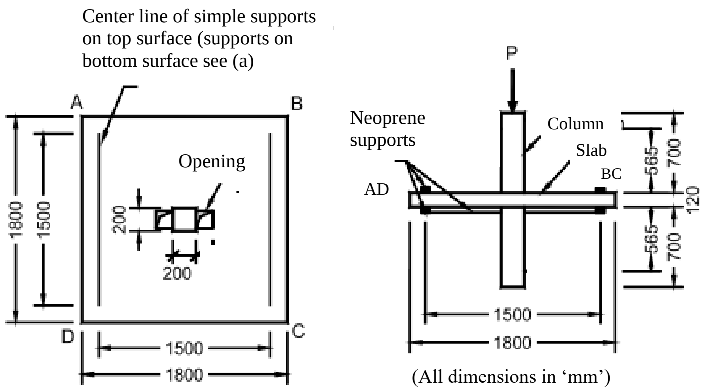

Figure 4. Specimen dimension [8]

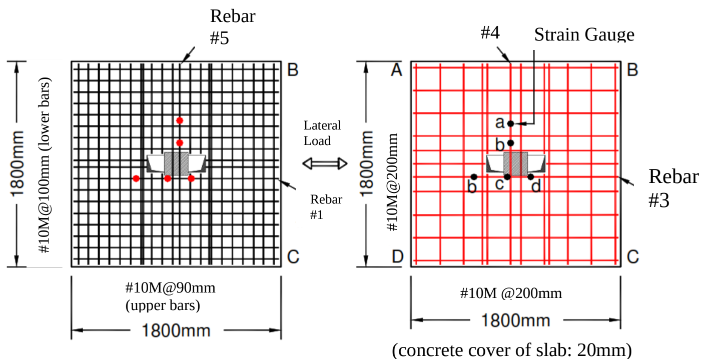

Figure 5. Specimen reinforcement arrangement [8]

Specimen SB1 used in this analysis is the interior connection tested under static loading through the column. SB1 had two square openings of 70 mm × 70 mm located besides the square column of 200 mm × 200 mm. Two layers of reinforcement were provided, bottom layer was 10M@100 and

10M@90. Top layer was 10M@200 in both directions (Fig. 5). The column was reinforced with four 15M bars and with 8M@115 mm ties. Compressive cylinder strength of concrete was $f_c' = 44$ MPa (according to ACI 318), and the tensile strength of concrete was $f_{cts} = 2.2$ MPa, obtained from the splitting tensile test. The yield strength of the reinforcing steel was 430 MPa.

3.2. Methodology

a. Simulation technique

The slab-column connection SB1 was simulated in ABAQUS [18]. Eight-noded hexahedral (brick) elements (C3D8R) were used for concrete with reduced integration to avoid the shear locking effect. 2-node linear truss elements (T3D2) were used to model reinforcements. Reinforcement was embedded inside concrete to simulate the bond between the concrete and the reinforcement, assuming the perfect bond.

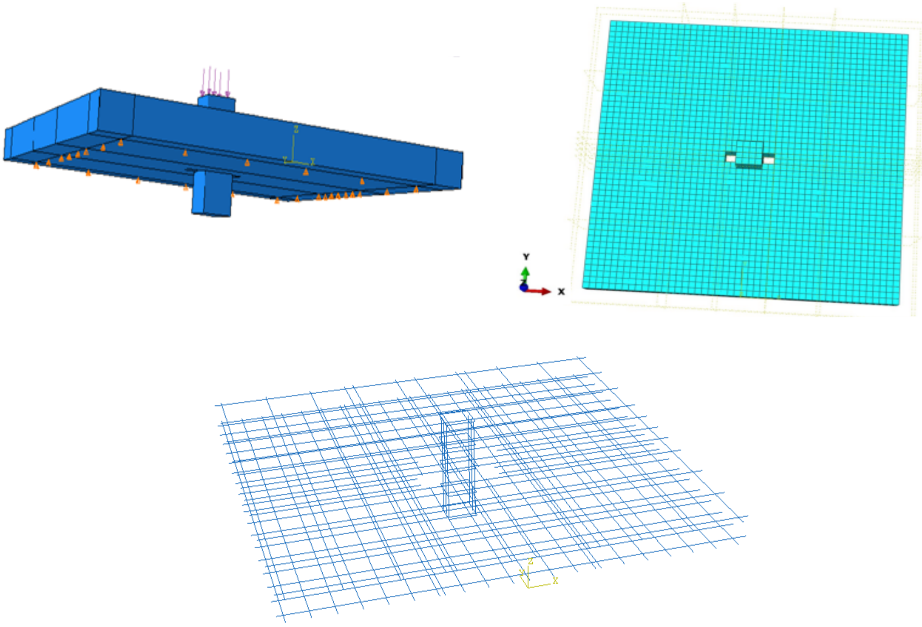

Figure 6. Simulation of SB1 specimen

Fig. 6 presents the modelling details including the geometry, the boundary conditions and meshing of specimen SB1 that were used for the simulation. In this analysis, a mesh size of 20 mm was used for both slab and column in vertical and horizontal directions. Therefore, through the slab thickness of 120 mm, six brick elements were used with all concrete elements having the same size of 20 mm.

A static analysis in ABAQUS/Explicit was adopted to analyse the control specimen SB1. A surface load was applied to the column and increased with a smooth amplitude curve from 0 to failure depending on the specific slab. Slab SB1 was applied with a loading rate of 20 kN/minute.

Restraint (UZ = 0) was introduced at the bottom edges of the specimen in the vertical direction. The summation of the reactions at the edges, where the boundary conditions were introduced, yielded the reactions equal to the punching shear loads.

b. Material models

Among the constitutive models for simulating the behavior of concrete, the concrete damaged plasticity model (CDP model) implemented in ABAQUS was adopted, and a short description of the model is presented herein.

The stress-strain response is illustrated in Fig. 7. In the CDP model, tension in concrete is defined by a stress-fracture energy approach proposed by Hillerborg [19]. He defines the energy required to open a unit area of crack, G_f, as a material parameter, using brittle fracture concepts. The implementation of this concept in a finite element model requires the definition of a characteristic length l_c associated with an integration point. This characteristic crack length l_c is based on the element geometry and formulation. It is used since the direction in which cracking occurs is not known in advance. In this study, the critical length l_c in the simulations is taken as 20 mm, which equals to the mesh size.

The Hognestad-type parabola is adopted for describing the compressive behavior of concrete (Fig. 7(b)).

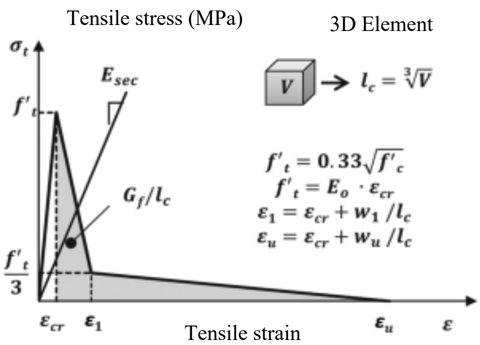

(a) Uniaxial tensile stress-strain relationship

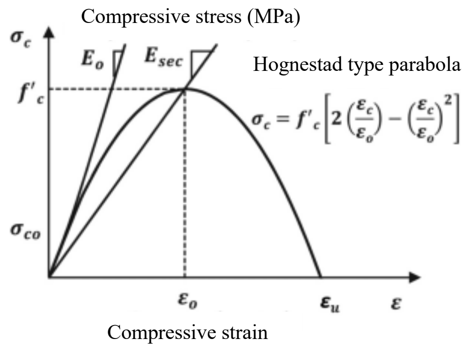

(b) Uniaxial compressive stress-strain relationship

Figure 7. Uniaxial stress-strain relationship of concrete of in CDP model

For reinforcement, the uniaxial stress-strain relationship is modeled with a bilinear strain hardening yield stress-plastic strain curve. The elastic behavior of the reinforcement is defined by specifying the Young's modulus of 200000 MPa and the Poisson's ratio of 0.3.

3.3. Model calibration

a. Crack development

Fig. 8 shows the crack development through the loading at 50%, 75% and 90% of the failure load at the slab bottom surface. At 50% of the failure load, many cracks appear in the vicinity of the column and few cracks exist in the diagonal direction from the column to the slab corners. As the load increases, at 75% of the failure load, the cracks develop further. Many diagonal cracks become more clearly, spreading from the column to the four coners. At 90% of the failure load, the cracks can be observed very clear. The plastic strain at the column edge is 0.00738.

b. Failure mode

Cracks appeared firstly in the vicinity of the column, then additional diagonal cracks developed towards four slab coners. When shear stress caused by the external load was greater than shear resistance of the slab, failure was occurred. It can be observed that the predicted failure mode from analysis is quite similar to that from the experimental test.

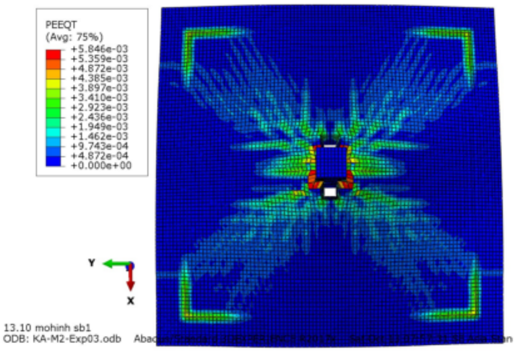

(a) 50% of failure load

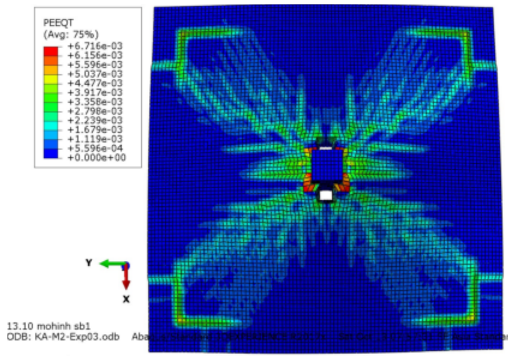

(b) 75% of failure load

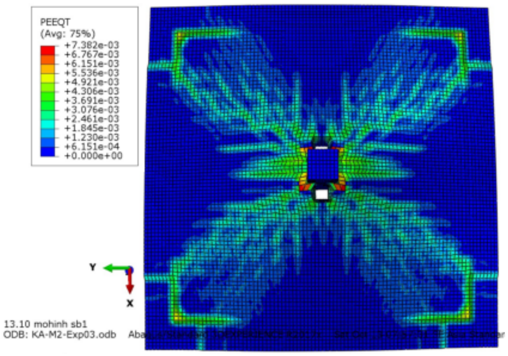

(c) 90% of failure load

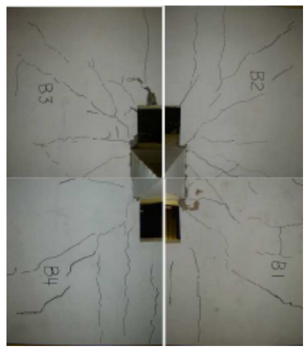

(d) Failure mode of typical specimen

Figure 8. Crack development at 50%, 75% and 90% of failure load at bottom surface

c. Load – displacement relationship

Fig. 9 shows the comparison of load – displacement curve at the specimen center between the experimental [8] and the numerical results. It shows that the load – displacement relationship is linear up to about 85 kN, at which the slab is in the elastic stage and no crack appears yet. In the experiment, as the load increased up to 65 kN, cracks developed and the curve was not linear anymore. When the load reached 232 kN, the slab was failed. In the simulation, the curve is more smooth than the experiment, but the model cannot converge when the load reaches 190 kN. This value is considered as the failure load in the analysis. In general, the simulation agrees well with the test results.

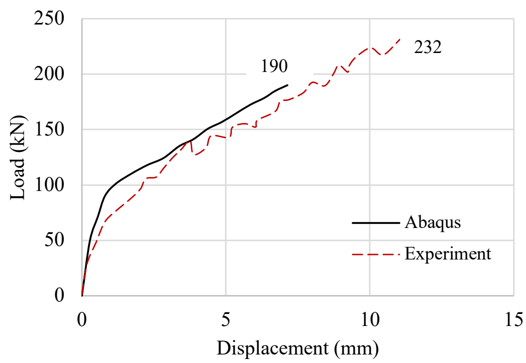

Figure 9. Load – displacement relationship at slab center

d. Punching shear resistance

The failure load from the Abaqus simulation is smaller than that of the experiment about 22%. This discrepancy can be explained by material nonlinearity and the convergence issue of the simulation. In the simulation, when reaching the so-called "failure" load of 190 kN, the model stops and cannot converge anymore. In the experiment, from that load (190 kN) onwards, cracks still developed toward the top surface of the slab. Thus, the slab was able to resist more load up to the failure load of 232 kN. Regarding the numerical convergence, a smaller mesh size had been tried but the result was not better. This is a shortcoming of the proposed model and should be improved in further study.

4. Parametric study

4.1. Investigated problems

Using the calibrated numerical model, an parametric study is conducted. The opening size and location are varied to investigate their effects on the punching shear resistance. The investigated problems are shown in Table 1. Three opening sizes of 70×70, 150×150 and 200×200 (in mm) located beside the column edge are investigated; while to study the effect of location, an opening of 70×70 is located at $0d$, $3d$ and $5d$ from the column edge, where d is the slab effective depth.

Table 1. Investigated problems in Abaqus

Model	Distance from column edge d = 90 mm	Opening size, mm
SB1	$0d$	70×70 150×150 200×200
SB2	$3d$	70×70
SB3	$5d$	70×70

4.2. Effect of opening size on punching shear resistance of flat slabs

Table 2 and Fig. 10 shows the numerical results of three different opening sizes located at a distance of $0d$ from the column edge. The simulation result from Genikomsou and Polak's study [8] is presented for comparison purpose. The concrete damaged plasticity model in Abaqus was adopted in their model. The punching shear resistance values predicted by ACI 318-19 and TCVN 5574:2018 are also presented.

Table 2. Comparison of punching shear resistance Pct with different opening sizes

Case	Simulation case	Reference model [8] (kN)	Proposed model (kN)	ACI 318-19 (kN)	TCVN 5574:2018 (kN)
1	70×70 (mm)	198	190	200.9	207.0
2	150×150 (mm)	161	156	169.4	174.6
3	200×200 (mm)	160	143	149.7	154.3

The punching shear resistance predicted by ACI 318-19 is taken as the minimum value of those calculated by Eqs. (5), (6), and (7). The effective depth d = 90 mm, the size effect factor $\lambda_s = 1$, and $\beta = 1$. The cylinder compressive strength f'_c is 44 MPa as given in [7], α_s is 40 for interior columns. For case 1, the critical perimeter is: $b_0 = 2 \times ((200 + 90) + (200 + 90)) - 2 \times 70 = 1020$ mm. The strength reduction factor ϕ is taken as 1.0, giving the punching shear resistance is 200.9 kN.

In accordance with TCVN 5574:2018, the punching shear resistance is calculated by Eq. (1), where the effective depth h_0 = 90 mm, the critical perimeter $u = 2\times((200+90)+(200+90))-2\times70$ = 1020 mm. It is noted that TCVN adopts the direct tensile strength R_{bt} in calculation, but both TCVN 5574:2018 and ACI 318-19 do not specify any relationship between the cylinder compressive strength and the direct tensile strength. In this paper the authors adopt the relationship proposed by Kim and Reda [20], which is $R_{bt} = f_t = 0.34\sqrt{f'_c}$ (MPa) = 2.26 MPa. The safety factor for tensile strength is taken as 1.0 for the comparison purpose. Thus, the punching shear resistance for case 1 in TCVN 5574:2018 is 207.0 kN.

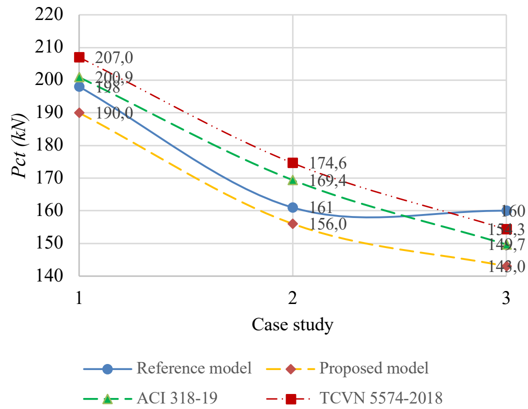

Figure 10. Punching shear resistance P_{ct} with different opening sizes

The calculation is done similarly for other cases, giving the results shown in Tables 2 and 3.

Table 3. Comparison of punching shear resistance P_{ct} with different locations

Case	Distance from the column edge	Reference model [8] (kN)	Proposed model (kN)	ACI 318-19 (kN)	TCVN 5574:2018 (kN)
4	0*d*	198	190.0	200.9	207.0
5	3*d*	207	191.8	221.6	228.3
6	5*d*	213	199.9	228.5	230.7

In the proposed Abaqus model, the punching shear resistance of case 1 (70×70 mm) is 190 kN; case 2 (150×150 mm) is 156 kN, reduced by 17.9%; and case 3 (200×200 mm) is 143 kN, decreased by 24.7% compared to case 1.

The predicted values in ACI 318-19 without the strength reduction factor of cases 1, 2 and 3 are 200.9 kN, 169.4 kN (reduced by 15.7%), and 149.7 kN (reduced by 25.5%), respectively. According to TCVN 5574:2018, the punching shear resistance values of case 1, 2, and 3 are 207.0 kN, 174.6 kN (reduced by 15.7%), and 154.3 kN (reduced by 25.5%), respectively.

It is obvious that as the opening sizes are increased the punching shear resistance is decreased since the control perimeter is reduced. When the opening is located right beside the column edge (0*d*), if the square opening size is about 1.3 times of the slab effective depth, the punching shear resistance is reduced by about 18%. If the square opening size is about 1.8 times of the slab effective depth, the punching shear resistance is reduced by about 25%.

On the other hand, the simulation values from Abaqus are only smaller than the predicted values by the codes about 9% (case 1) to 12% (case 2). Therefore, the proposed numerical model can be reliable. ACI 318-19 and TCVN 5574:2018 give very close prediction, only difference of 3%. This is because TCVN 5574:2018 takes the critical section at distance of $0.5h_0$ and also count for the reduced control perimeter if the opening is presented, similar concepts with ACI 318-19. It is a novelty of this 2018 version compared to the 2012 version of TCVN.

4.3. Effect of opening location on punching shear resistance of flat slabs

Table 3 summarises the punching shear resistance predictions by the reference and proposed numerical models, by ACI 318-19 and TCVN 5574:2018 for the opening size of 70×70 at the different locations (at a distance of $0d, 3d, 5d$ from the column edge).

According to ACI 318-19, the prediction values without the strength reduction factor are 200.9 kN, 221.6 kN (increased by 10.3%) and 228.5 kN (increased by 13.7%) for case 4, 5 and 6, respectively. It should be noted that when the opening is located further than $4h$, it is not necessary to reduce the critical perimeter.

When the opening is located at $0d$, TCVN 5574:2018 prediction is 207.0 kN since the opening is within the punching shear cone. At the locations of $3d$ and $5d$, the punching shear resistance values are 228.3 kN and 230.7 kN, respectively (an increase of 10.3% and 11.4%).

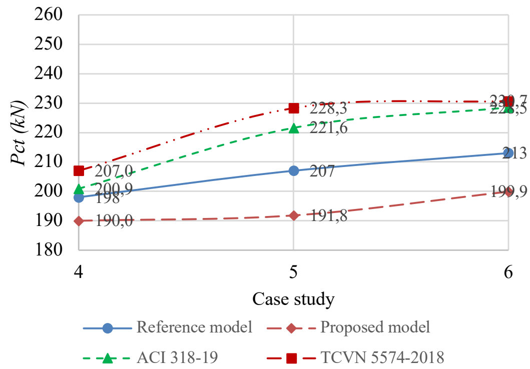

Figure 11. Punching shear resistance P_{ct} with the opening located at $0d, 3d, 5d$

The prediction values in the proposed numerical model are although in a good agreement with those from the reference model, but not good as in cases 1, 2 and 3. Comparison of the numerical results with those calculated from the two building codes give a maximum discrepancy of about 19% (case 5). This can be caused by the convergence issue of the numerical model. This should be improved in further study.

Once again, the calculated values from ACI318-19 and TCVN 5574:2018 are in a very good agreement since the design principles of these two codes are very similar.

From the study, two design recommendations can be withdrawn as follows:

- If the opening length is greater than the width of the critical perimeter at one column edge, that edge shall be considered as a free edge. As a result, the openings should be only located at one or two sides of the column edges.

- In regard to the opening location, the recommendation in ACI 318-19 could be used instead of that in TCVN 5574:2018. If the shortest distance between the perimeter of the loaded area (column) and the edge of the opening is greater than $4h$, there is no need to consider any reduction of the critical perimeter.

5. Conclusions

This paper introduces a proposed numerical model using Abaqus that is enable to simulate the behaviour of punching shear of flat slabs with openings. The model is validated well with the previous test data and give a good prediction of punching shear resistance, showing that the model can be reliable. However, some improvements on the proposed model are still required.

Using the validated numerical model, the effects of opening size and location on the punching shear resistance of flat slabs are then investigated. When the opening is located right beside the column edge ($0d$), if the square opening size is about 1.3 times of the slab effective depth, the punching shear resistance is reduced by about 18%. If the square opening size is about 1.8 times of the slab effective depth, the punching shear resistance is reduced by about 25% to 30%. With the same opening size, as its distance from the column edge is increased, the punching shear resistance is increased.

The punching shear resistances calculated by ACI 318-19 and TCVN 5574:2018 with different opening sizes and locations are agreed well, since the design principles between two codes now are similar.

Acknowledgements

The research presented in this paper was funded by Ministry of Construction (MOC Vietnam) under Grant no. RD 68-20. The financial support of MOC is gratefully acknowledged.

References

[1] Aurelio, M. (2008). Punching Shear Strength of Reinforced Concrete Slabs without Transverse Reinforcement. *ACI Structural Journal*, 105(4).

[2] Ramos, A. P., Lúcio, V. J. G. (2008). Post-punching behaviour of prestressed concrete flat slabs. *Magazine of Concrete Research*, 60(4):245–251.

[3] Han, S.-W., Park, Y.-M., Kee, S.-H. (2009). Stiffness Reduction Factor for Flat Slab Structures under Lateral Loads. *Journal of Structural Engineering*, 135(6):743–750.

[4] Elstner, R. C., Hognestad, E. (1956). Shearing Strength of Reinforced Concrete Slabs. *ACI Journal Proceedings*, 53(7):29–58.

[5] Moe, J. (1961). *Shearing strength of reinforced concrete slabs and footings under concentrated loads*. Development Department Bulletin D47, Portland Cement Association: Skokie, Illinois.

[6] ACI 318-19 (2019). *Building code requirements for structural concrete and Commentary*. American Concrete Institute.

[7] Genikomsou, A. S., Polak, M. A. (2015). Finite element analysis of punching shear of concrete slabs using damaged plasticity model in ABAQUS. *Engineering Structures*, 98:38–48.

[8] Genikomsou, A. S., Polak, M. A. (2017). Effect of Openings on Punching Shear Strength of Reinforced Concrete Slabs—Finite Element Investigation. *ACI Structural Journal*, 114(5).

[9] Mostofinejad, D., Jafarian, N., Naderi, A., Mostofinejad, A., Salehi, M. (2020). Effects of openings on the punching shear strength of reinforced concrete slabs. *Structures*, 25:760–773.

[10] Hieu, P. T. (2019). *Study on punching shear resistance of reinforced concrete flat slabs using ultra-high performance concrete*. Hanoi University of Civil Engineering.

[11] Vuong, P. N. (2018). *Analysis of punching shear resistance of reinforced concrete flat slabs considering the boundary conditions using Ansys*. National University of Civil Engineering: Department of post-graduate studies.

[12] Tam, T. V. (2019). *Study on punching shear resistance of prestress concrete flat slabs*. National University of Civil Engineering: Department of post-graduate studies.

[13] Vinh, T. X., Hieu, N. T., Dat, P. X., Hung, N. M. (2021). Evaluation of punching shear capacity of two-way RC slabs without transverse reinforcement according to different provisions. *Journal of Science and Technology in Civil Engineering (STCE) - HUCE*, 15(3):171–184.

[14] Viet, V. Q., Ha, H., Hoan, P. T. (2019). Evaluation of ultimate bending moment of circular concrete–filled double skin steel tubes using finite element analysis. *Journal of Science and Technology in Civil Engineering (STCE) - HUCE*, 13(1):21–32.

[15] Phan, H. D. (2021). Numerical analysis of seismic behavior of square concrete filled steel tubular columns. *Journal of Science and Technology in Civil Engineering (STCE) - HUCE*, 15(2):127–140.

[16] TCVN 5574:2018. *Concrete and reinforced concrete structures - Design standard*. Ministry of Science and Technology.

[17] TCVN 5574:2012. *Concrete and reinforced concrete structures - Design standard*. Ministry of Science and Technology.

[18] ABAQUS (2010). *Analysis User's Manual 6.10*. Dassault Systems Simulia Corp.: Providence, RI.

[19] Hillerborg, A., Modéer, M., Petersson, P.-E. (1976). Analysis of crack formation and crack growth in concrete by means of fracture mechanics and finite elements. *Cement and Concrete Research*, 6(6):773–781.

[20] Kim, J. J., Taha, M. R. (2014). Experimental and Numerical Evaluation of Direct Tension Test for Cylindrical Concrete Specimens. *Advances in Civil Engineering*, 2014:1–8.